European Journal of Soil Science

European Journal of Soil Science, Volume 65, Issue 2, Pages 248–263, March 2014

Assessment of soil organic carbon at local scale with spiked NIR calibrations: effects of selection and extra-weighting on the spiking subset

Journal:	*European Journal of Soil Science*
Manuscript ID:	EJSS-060-13.R1
Manuscript Type:	Original Manuscript
Date Submitted by the Author:	24-Aug-2013
Complete List of Authors:	Guerrero, César; Universidad Miguel Hernandez de Elche, Agroquímica y Medio Ambiente Stenberg, Bo; Swedish University of Agricultural Sciences, Soil and Environment Wetterlind, Johanna; SLU, Department of Soil and Environment Viscarra Rossel, Raphael; CSIRO, Land and Water Maestre, Fernando; Universidad Rey Juan Carlos, Departamento de Biología y Geología Mouazen, Abdul Mounem; National Soil Science Institute, Natural Resources Department Zornoza, Raul; Universidad Politécnica de Cartagena, Departamento de Ciencia y Tecnología Agraria Ruiz-Sinoga, Jose Damian; Universidad de Málaga, Departamento de Geografía Kuang, Boyan; Cranfield University, Natural Resources Department
Keywords:	SOC assessment, soil sensing, near infrared spectroscopy, spiking, extra-weighting

Assessment of soil organic carbon at local scale with spiked NIR calibrations: effects of selection and extra-weighting on the spiking subset

C. GUERRERO[A], B. STENBERG[B], J. WETTERLIND[B], R.A. VISCARRA ROSSEL[C], F.T. MAESTRE[D], A.M. MOUAZEN[E], R. ZORNOZA[F], J.D. RUIZ-SINOGA[G] & B. KUANG[E]

[a]*Departamento de Agroquímica y Medio Ambiente, Universidad Miguel Hernández de Elche, E-03202, Spain,* [b]*Department of Soil and Environment, SLU, Skara, Sweden,* [c]*CSIRO Land and Water, Canberra, Australia,* [d]*Departamento de Biología y Geología, Universidad Rey Juan Carlos, Spain,* [e]*Department of Environmental Science and technology, Cranfield University, UK,* [f]*Departamento de Ciencia y Tecnología Agraria, Universidad Politécnica de Cartagena, Spain, and* [g]*Departamento de Geografía, Universidad de Málaga, Spain.*

Correspondence: César Guerrero. E-mail: cesar.guerrero@umh.es

Running title: Spiking and extra-weighting to improve soil organic carbon predictions with NIR

Summary

Spiking is a useful approach to improve the accuracy of regional or national spectroscopic calibrations when they are used to predict at local scales. To do this, a small subset of local samples (spiking subset) is added to recalibrate the regional or national calibration. If the spiking subset is small in comparison with the size of the initial calibration set, then the spiking subset could have little noticeable effect and only a small improvement can be expected. For these reasons, we hypothesised that the accuracy of the spiked calibrations can be improved when the statistical relevance of the spiking subset is given extra-weight. We also hypothesised that the spiking subset selection and the initial calibration size were relevant, and could affect the accuracy of the recalibrated models. To test these hypotheses, we evaluated different strategies to select the best spiking subset, with and without extra-weighting, to spike three initial calibrations of different sizes. These calibrations were used to predict the soil organic carbon (SOC) content in samples from four target sites. Our results confirmed that spiking improved the prediction accuracy of the initial calibrations. We observed differences in accuracy depending on the spiking subset used. The best results were obtained when the spiking subset contained local samples evenly distributed in the spectral space, regardless of the initial calibration's characteristics. The accuracy was significantly improved when the spiking subset was extra-weighted. For medium- and large-sized initial calibrations, the improvement due to extra-weighting was larger than that caused by the increase in spiking subset size. This result is interesting because extra-weighting the spiking subset is an inexpensive task. Similar accuracies were obtained using small- and large-sized initial calibrations, suggesting that incipient spectral libraries could be useful if the spiking subset is properly selected and extra-weighted. When small-sized spiking subsets were used, the predictions results were

more accurate than those obtained with 'geographically local' models. Overall, our results indicate that we can minimise the efforts needed to effectively use near-infrared (NIR) spectroscopy for SOC assessment at local scales.

Keywords: SOC assessment, soil sensing, near infrared spectroscopy, spiking, extra-weighting.

Introduction

Using near-infrared (NIR) spectroscopy to estimate soil properties is rapid, non-destructive and relatively inexpensive compared to conventional laboratory analyses, particularly when processing many samples. For NIR spectra to be quantitatively useful, we need to develop and use a soil spectral database or library to derive spectroscopic models (calibrations) that relate the spectra to analytical data, e.g. soil organic carbon (SOC). When assessing soil properties at a local scale, we can develop site-specific or 'geographically local' calibrations (Wetterlind *et al.*, 2010) that are generally very accurate because smaller areas tend to be less variable in terms of the dependent variable (Stenberg *et al.*, 2010), and the samples used to develop the calibration and those used for prediction share similar characteristics, such as mineralogy and organic matter quality (Reeves *et al.*, 1999; Janik *et al.*, 2007; Guerrero *et al.*, 2010; Wetterlind *et al.*, 2010). A disadvantage of these models is that they are only valid for the local area, which could be an expensive strategy when evaluating multiple areas. Another option is to use regional, national or global calibrations, but they should represent the variability of the soils being analysed. This has caused a trend to develop larger-scale calibrations with a very large number of samples to ensure that the local samples fall

within the model's domain (Shepherd & Walsh, 2002; Brown *et al.*, 2006; Viscarra Rossel, 2009; Grinand *et al.*, 2012; Viscarra Rossel & Webster, 2012), although this cannot be guaranteed because soils have such variable characteristics, even at a regional scale. Furthermore, a set of samples comprising a large-scale calibration should be considered heterogeneous, but the local samples could be considered as a homogeneous set that is located in a small area of the overall calibration domain. This could be the reason for inaccurate (biased) results observed by some authors when using regional and national calibrations to make predictions at local scales (Brown *et al.*, 2005; Brown, 2007; Janik *et al.*, 2007; Christy, 2008; Sankey *et al.*, 2008; Guerrero *et al.*, 2010; Stenberg *et al.*, 2010; Wetterlind & Stenberg, 2010), even when the local samples fall within the model domain and are not recognised as outliers. This could also explain why better results are obtained with local (spectrum-specific) models (Genot *et al.*, 2011; Gogé *et al.*, 2012), where a subset of library samples that are similar to the unknown sample is used to construct the calibration (Pérez-Marín *et al.*, 2007). However, local methods are expensive because a large spectral library is needed to find sufficient similar samples for the calibrations.

Spiking is an alternative method proposed to improve the accuracy of regional or national calibrations for use at local scales (Viscarra Rossel *et al.*, 2009; Guerrero *et al.*, 2010; Stenberg *et al.*, 2010; Wetterlind & Stenberg, 2010; Kuang & Mouazen, 2013). Spiking—sometimes referred to as 'augmentation' (Brown *et al.*, 2006; Brown, 2007; Sankey *et al.*, 2008) and other names—involves three main steps (Janik *et al.*, 2007). First, analyse a few samples from the target site in the laboratory using the reference method; then add these samples to the initial calibration matrix; and then recalibrate the model. This procedure usually increases the accuracy of the predictions in the rest of the samples from the target site (Brown *et al.*, 2005; Sankey *et al.*, 2008; Wetterlind &

Stenberg, 2010). The higher the number of local samples in the spiking subset, the higher the accuracy in the prediction set (Brown, 2007; Guerrero *et al.*, 2010), but a large spiking subset decreases the advantages of NIR spectroscopy as a quick and low-cost analytical method. To increase the relative proportion of the spiking subset, Guerrero *et al.* (2010) suggested decreasing the number of samples in the initial calibration set because they obtained higher accuracies when small-sized calibrations were spiked, where the spiking subset had a larger influence. However, the selection of a small number of calibration samples can reduce the amount of important information for modelling, and lead to less robust calibrations. For this reason, we proposed an alternative approach to increase the relevance of the spiking subset in the NIR calibrations. The approach is to increase the statistical weight of the spiking subset by adding several copies of the subset to the calibration matrix. These extra-weighted samples are more important than other samples used to form the statistical model (Capron *et al.* 2005; Stork & Kowalski 1999), which forces the calibration to better fit the extra-weighted samples. If these samples were similar to the overall prediction set, the model should provide more accurate predictions. We also evaluated different strategies to select the best spiking subset. Since each local sample is different to the others, we hypothesised that the selection of a spiking subset would influence the accuracy of the spiked models, and the selection would be more influential if fewer samples were used for spiking.

The spiking approach tries to gain benefits from a previously developed or initial large-scale calibration set. It is reasonable to assume that results obtained could be affected by the characteristics of the initial calibration, as some authors observed (Guerrero *et al.*, 2010; Wetterlind & Stenberg, 2010). For this reason, we included different initial calibrations in this study and evaluated their influence on the spiking

process. Our first objective was to evaluate how local samples should be selected as a spiking subset for optimal spiking. To do this, we compared thirteen different strategies to select the samples for the spiking subset. Our second objective was to evaluate whether an extra-weighted spiking subset increased the prediction accuracy. In addition, we compared geographically local models that used three different sized spiking subsets. We selected SOC as the soil property for prediction, and we used the coefficient of determination (R^2), root mean square error of prediction (RMSEP), standard error of prediction (SEP) and ratio of performance to deviance (RPD) to evaluate the prediction performance for four different target sites.

2. Material and methods

2.1. National samples and initial calibrations

A national soil library (n = 2836) of soils from different sites across Spain (predominantly southeastern Spain) was randomly split into three subsets. These subsets were used to create three initial calibrations of different sizes, representing three different stages or efforts to develop the spectral library: small (IC#1; n = 192), medium (IC#2; n = 365) and large (IC#3; n = 2279). The soils in the soil library were collected under forest and agricultural land uses. Most of these soils developed over sedimentary (mostly calcareous) lithologies. The soil samples were air-dried and sieved (< 2 mm), and the NIR spectra (12 000–3800 cm^{-1}) were obtained by FT–NIR diffuse reflectance spectroscopy (MPA, Bruker Optik GmbH, Germany). The scale of the spectra was transformed to nanometers (830–2630 nm), and re-sampled to 1 nm resolution. The SOC concentration (%) was determined using the Walkley & Black (1934) method. The different initial calibrations, relating the SOC to the NIR spectra, were constructed

using partial least squares (PLS) regression (PLS-1 algorithm) (see section 2.6 for details). Key characteristics of the initial calibrations are shown in Table 1.

2.2. Target sites

We selected four independent target sites from four regions with spectral characteristics that differed from each other and from those observed in the initial calibrations (Figure 1; Appendix 1). Each target site is a relatively small area of dense sampling, from several hectares to a few square kilometres in size. A different number of local samples were collected at each target site (Table 2). One site was located in Sweden (TS1), two in Spain (TS2, TS3) and one in the United Kingdom (TS4). As with the initial calibration samples, the soil samples from the target sites were air-dried and sieved (< 2 mm), and the NIR spectra and SOC content were obtained. Most of the spectra were collected using a FT–NIR (MPA, Bruker Optik GmbH, Germany), except the TS1 samples, which were scanned using a vis–NIR (ASD FieldSpec Pro Fr, USA). The scale of the FT–NIR spectra was transformed from cm^{-1} to nanometers, and re-sampled to 1 nm. For details about FT–NIR and vis–NIR scanning, see Guerrero *et al.* (2010) and Wetterlind & Stenberg (2010), respectively.

2.3. Calibration types

Different types of calibrations relating SOC and NIR spectra were obtained using PLS as a regression method (see section 2.6), and were used to predict the SOC contents in the target site samples.

Initial calibrations: three different-sized initial calibrations (IC#1, IC#2 and IC#3, described in section 2.1) that did not contain any samples from the target sites; referred to as unspiked initial calibrations (Figure 2a; section 2.6).

Spiked calibrations: the three initial calibrations modified by adding a spiking subset (n = 8) (Figure 2b). We used 13 different spiking subsets to spike each of the initial calibrations (see section 2.4). In each initial calibration, we obtained 13 subtypes of spiked calibrations, and we repeated this procedure for each of the four target sites.

Spiked calibrations with extra-weighting: in each of the different spiked calibrations, the spiking subset was extra-weighted. To do this, we added 24 copies of each spiking subset sample to the calibration set (Figure 2c), and then recalibrated the model (see section 2.6). Each of the eight spiking subset samples appears 25 times in the calibration matrix, becoming 24 times more influential than the soil library samples because we have modified their leverage (Stork & Kowalski, 1999). We selected 24 copies because the leverage of the target site samples followed an asymptotic pattern after the addition of 15–20 copies (data not shown).

2.4. Strategies to select the spiking subset from the target site samples

For each target site, we used 13 strategies to select the different types of spiking subsets. We hypothesised that each strategy had different advantages. The strategies were designed and grouped on the basis of (i) the SOC values of target site samples, (ii) the spectral characteristics of the target site samples and (iii) the spectral relationships between the initial calibrations and the target site samples using the Mahalanobis distance values. The first group of five strategies was designed on the basis of the SOC content of target site samples. These strategies have a strictly theoretical value for interpreting some results because the SOC contents of the target site samples would be unknown in a real scenario, and thus these strategies would not be useful in practice.

Strategy 1 (OC low): select eight target site samples with the lowest SOC values (left tail of SOC histogram). Samples with low SOC contents will show more clearly the

spectral features of the inorganic constituents, which are the most important factors impeding the use of a calibration from one site to another. Moreover, these samples could be useful to correct the bias in target site samples with low SOC contents.

Strategy 2 (OC high): select eight target site samples with the highest SOC values (right tail of SOC histogram). These samples mask the inorganic spectral features, and clearly show the SOC spectral features in the local samples. Moreover, these samples can be useful to correct bias in target site samples with high SOC contents.

Strategy 3 (OC tails): select four samples with the lowest SOC values (from the left tail of the SOC histogram) and four with the highest SOC values (from the right tail). These samples can be useful to correct bias because the low and high SOC contents are well established. Since low and high values are well described, the offset should be also corrected.

Strategy 4 (OC centre): select eight target site samples with SOC values around the median SOC value of the set.

Strategy 5 (OC distrib): select eight target site samples at regular intervals over the entire range of SOC values (samples evenly distributed across the SOC values). These samples should also be adequate for bias and offset correction.

To apply the three strategies in the second group, we performed a principal component analysis (PCA) of the target site samples (NIR spectra pre-processed with Savitzsky–Golay first derivative). The scores of the first, second and third principal components (i.e. the first three) are represented in a scatter-plot.

Strategy 6 (PC periph): select eight target site samples located at the periphery of the principal component spectral space defined by the first three principal components.

Strategy 7 (PC centre): select eight target site samples located at the centre of the principal component spectral space defined by the first three principal components. These are the most similar samples to the mean spectrum of the target site spectra.

Strategy 8 (PC distrib): select eight target site samples evenly distributed across the principal component spectral space defined by the first three principal components. This is the most intuitive strategy to uniformly cover the spectral diversity. This selection was made using the 'Automatic selection subset' option in OPUS (version 6.5 software; BrukerOptik GmbH, Ettlingen, Germany), which selects samples in a similar fashion to the Kennard–Stone algorithm (Kennard & Stone, 1969).

The third group of five strategies was based on the Mahalanobis distance values of the target site samples. The Mahalanobis distance values were calculated with respect to the unspiked initial calibrations. Each target site sample had a different Mahalanobis distance depending on the initial calibration used (i.e. IC#1, IC#2 or IC#3).

Strategy 9 (MD low): select eight target site samples with the lowest Mahalanobis distance values (left tail of Mahalanobis distance histogram). These target site samples are the closest to the initial calibration samples and the overall target site samples, and could become a 'bridge' between both sets.

Strategy 10 (MD high): select eight target site samples with the highest Mahalanobis distance values (right tail of Mahalanobis distance histogram). These samples are the first recognised as outliers. In some schemes of calibration maintenance (Shepherd & Walsh; 2002), it has been suggested the addition of this type of samples when calibrations must be updated. These target site samples are the most effective decreasing the Mahalanobis distance of the overall target site set (Capron *et al.*, 2005).

Strategy 11 (MD tails): select four target site samples with the lowest Mahalanobis values and four with the highest Mahalanobis distance values.

Strategy 12 (MD centre): select eight target site samples with Mahalanobis distance values around the median Mahalanobis distance value.

Strategy 13 (MD distrib): select eight target site samples at regular intervals over the entire range of Mahalanobis distance values (samples evenly distributed across the Mahalanobis distance values).

2.5 Experimental design and statistical analysis

For this study, a repeated measures factorial design was established. The between-subject factors were 'initial calibration', with three levels (i.e. three initial calibrations of different sizes, IC#1, IC#2 and IC#3) and 'strategy', with 13 levels (i.e. 13 spiking subset selection strategies). The within-subject factor was 'extra-weighting', with two levels (i.e. without and with extra-weighting). For each combination of factors, we calculated the R^2, RMSEP, SEP and RPD to compare the actual SOC content of the target site samples with the SOC predicted by the different calibrations. This design was applied separately to the four target sites. The prediction performance parameters obtained in each target site were considered as replicates. We used RMSEP to inform us about accuracy and SEP about precision. The RPD (the ratio between the standard deviation of the prediction set and the RMSEP) allowed us to compare the accuracy obtained in prediction sets with different standard deviations.

The differences in RMSEP, SEP and RPD were analysed using a repeated measures ANOVA. We excluded the strategies based on the SOC values (strategies 1–5) from the statistical analysis because they are not useful in practice. In this way, the repeated measures ANOVA was performed using eight levels of spiking subset selection strategy

and three levels of initial calibration as the between-subject factors, and two levels of extra-weighting as the within-subject factor. Homocedasticity and normality was checked using Levene and Kolmogorov–Smirnov tests, respectively; the original variables were transformed to meet with the ANOVA assumptions when appropriate. The R^2 was excluded from this statistical analysis because it did not meet the assumptions. The assumption of sphericity was not violated when using the Mauchly's test of sphericity. The software IBM SPSS Statistics version 20 (IBM, Armonk, NY) was used for statistical analyses. We also obtained predictions using the unspiked initial calibrations, but these results were not included in the statistical analysis.

2.6. Development of calibrations with PLS-regression

The models relating the NIR spectra with the SOC contents in soils were obtained with PLS-regression (PLS-1 algorithm; OPUS version 6.5 software; BrukerOptik GmbH, Ettlingen, Germany). We selected the number of PLS-vectors through leave-one-out cross-validation. Before calibration, the SOC contents were transformed by the square root but predicted SOC data were back-transformed before we compared them with actual SOC and calculated the prediction performance parameters. NIR-spectra were transformed by the first derivative (Savitzsky–Golay, 25 points). The number of PLS-vectors in the spiked calibrations was set to the same number as in the corresponding initial calibration. In TS1, we used the spectral range 1000–2500 nm to meet a common range with a similar noise to the spectra collected with the FT-NIR instrument.

2.7. Additional comparisons: extra-weighting effect versus the increase of the spiking subsets size and versus geographically local models

These comparisons were made only with spiking subsets selected by the ‘PC distrib’ strategy, which was one of the most effective selection strategies in terms of increasing

accuracy. We compared the extra-weighting effect against the increase of the spiking subsets size. To do this, we spiked the three initial calibrations with 8, 16 and 32 spiking subset samples selected by the 'PC distrib' strategy. Similar to the procedure described in section 2.3, we obtained spiked calibrations by adding 24 copies of the spiking subset (denoted as EW_24). For each target site, we used these calibrations to predict the SOC contents in the target site samples. In all cases, the 32 spiking subset samples were not used in the RMSEP computation, to allow a fair comparison of accuracy regardless of the size of the spiking subset. The RMSEP values were analysed with a repeated measures ANOVA, where two levels of extra-weighting (with and without extra-weighted) acted as the within-subject factor, and three levels of the spiking subsets size (8, 16 and 32 samples) acted as the between-subject factor. Due to the large differences between the sizes of the initial calibrations, we also used a different approach to calculate the number of copies to add, which was the ratio between the initial calibration size and the spiking subset size. In this way, more copies are added when the initial calibration size is larger or when the spiking subset size is smaller. The extra-weighting effect obtained using the initial calibration-to-spiking subset ratio (denoted as EW_ratio) was evaluated using repeated measures ANOVA, as for the EW_24 approach. The data used in these statistical analyses did not violate the ANOVA assumptions (homocedasticity and normality) or the condition of sphericity. For each target site, three geographically local or site-specific models were constructed using the 8, 16 and 32 spiking subsets selected by the 'PC distrib' strategy.

3. Results

3.1. Effect of spiking (without extra-weighted)

The predictions obtained with the unspiked initial calibrations for each target site were inaccurate, with large prediction errors (Figure 3). For the 12 cases (three initial calibrations applied to four target sites), the RPD values ranged from < 0.10 to 1.44, which clearly indicated poor predictions. Figure 4 shows the R^2, RMSEP, SEP and RPD values obtained with the unspiked and spiked calibrations, where each value shown is the mean value of those obtained for the four target sites. The unspiked IC#1 provided very low quality predictions, with $R^2 = 0.33 \pm 0.34$ (mean ± standard deviation) and RPD = 0.52 ± 0.21 (Figure 4a). Once spiked, we observed a drastic and positive change in all the parameters related to the quality of predictions (Figure 4a), and bias was substantially decreased. There were differences in accuracy for the spiked calibrations depending on the strategy used to select the spiking subset. For example, the RMSEP values obtained with the IC#1 spiked using the 'OC low'(worst) and 'PC distrib'(best) strategies were 0.70 ± 0.16% and 0.37 ± 0.15% SOC, respectively, both of which were clearly better than the RMSEP for the unspiked IC#1 of 1.86 ± 1.77% SOC (Figure 4a). Similarly, spiking of IC#2 (Figure 4b) caused a noticeable improvement in prediction accuracy, mostly due to improvement of bias. Interestingly, the worst ('OC low') and best ('PC distrib') strategies for IC#2 were the same as those observed for IC#1. A substantial improvement in accuracy was also obtained when IC#3 was spiked, due to a strong decrease in bias (Figure 4c). In this case, the worst and best strategies (in terms of accuracy) were not the same as for IC#1 and IC#2. In general, the best accuracies were obtained using IC#1 (the calibration with the smallest size) and the worst accuracies were obtained with IC#3 (the calibration with the largest size). To illustrate the effect of spiking with different spiking subsets, individual results for the four target sites obtained with the 'MD centre' and 'PC distrib' selection strategies are shown in Figure 3.

3.2. Effect of extra-weighting on the spiking subset selection strategies

The addition of several copies of the spiking subset (i.e. extra-weighting) in the spiked calibrations caused a significant improvement ($P < 0.001$) in the RMSEP, SEP and RPD (Table 3). The effect of extra-weighting on these parameters was similar across the spiking subset selection strategies (extra-weighting × strategy, $P > 0.05$; Table 3), and also similar in the three different initial calibrations evaluated (extra-weighting × initial calibration, $P > 0.05$; Table 3), although the extra-weighting effect on the R^2 was greater in IC#3 (Figure 4).

We observed that accuracy differed depending on the strategy used to select the spiking subset (Figure 4). Indeed, all the parameters evaluated showed significant differences across the strategies (Table 3). The differences between strategies were similar in the three initial calibrations evaluated, as suggested by the non-significant interaction between the 'strategy' and the 'initial calibration' ($P > 0.05$; Table 3). In two strategies ('OC low' and 'OC high'), extra-weighting had a negative effect through an increase in bias (Figure 4). The 'OC low' strategy was worst for IC#2 and IC#3, and second worst for IC#1. When extra-weighting was applied, 'PC distrib' was the best performing strategy in the three initial calibrations, and clearly improved the accuracy due to decrease in bias, but also due to a decrease in SEP (Figure 3 & Figure 4). In IC#1 and IC#2, the combined use of the spiking subset ('PC distrib') and extra-weighting increased the RPD by 1.5 units compared to the unspiked initial calibrations, allowing RPD values to exceed 2 (Figure 4). The results obtained with the 'MD centre' and 'PC distrib' strategies (without and with extra-weighting) for each target site illustrate the extra-weighting effects (Figure 3).

3.3. Increase of spiking subsets size versus extra-weighting, and comparison with geographically local models

We compared the effects of increasing the spiking subset size with extra-weighting for the 'PC distrib' selection strategy. There was a positive effect on the accuracy when the spiking subset size was increased (Figure 5), although this effect was not significant ($P > 0.05$; Table 4). Regardless of the spiking subset size, there was a significant improvement in the accuracy when the spiking subsets were extra-weighted ($P < 0.001$, Table 4). These results were similar for the two approaches followed to select the number of copies to add for extra-weighted (Table 4, Figure 5). It is worth highlighting that in IC#2 and IC#3, the improvement of the accuracy due to extra-weighting was clearly higher than the duplication of the spiking subset size (Figure 5), and even higher than the quadruplication of the spiking subset size in IC#3 (Figure 5). The extra-weighting effect in IC#1 was smaller because spiking was enough to cause the saturation of the improvement, mainly due to it smaller size. When the spiking subset was not extra-weighted (black bars in Figure 5), the best results were obtained with the small-sized initial calibration (IC#1), and results obtained with IC#2 and IC#3 were less accurate than those obtained with the geographically local models. Once the spiking subset was extra-weighted, the differences between initial calibrations practically disappeared, especially when the number of copies added was selected according to the ratio of the initial calibration to the spiking subset (EW_ratio; light grey bars in Figure 5). When this approach was used for extra-weighting (EW_ratio), the spiked initial calibrations were more accurate than the geographically local models. When a large number of local samples (32) were considered as spiking subset size (SS = 32), and also as 'n' of the geographically local models (n = 32), scarce differences between both approaches were observed, except for the reduced robustness obtained with the geographically local models (Figure 5).

4. Discussion

4.1. Effect of spiking

The predictions obtained using the unspiked initial calibrations had a low accuracy. The bias was the main problem, representing more than 50% of the error, as some authors observed (e.g. Bellon-Maurel & McBratney, 2011). These results were expected, and clearly demonstrate how we cannot safely used calibrations do not cover the characteristics of the target sites. As for any model, the spectroscopic calibrations are valid only for samples with similar characteristics as those used in the calibration (Viscarra Rossel *et al.,* 2008). For these reasons, there is a trend to develop large spectral libraries (Shepherd & Walsh, 2002; Brown *et al.*, 2006; Viscarra Rossel, 2009; Grinand *et al.*, 2012; Viscarra Rossel & Webster, 2012). But the accuracy of the calibrations improved drastically when only eight local samples were added to spike the initial calibrations. Once the calibrations contained relevant information for the target site, the predictions became more accurate. The improved accuracy was mostly due to the decrease in bias, in accordance with previous studies (e.g. Stork & Kowalski, 1999; Bricklemyer & Brown, 2010; Guerrero *et al.,* 2010; Stenberg *et al.,* 2010; Wetterlind & Stenberg, 2010), but also by an improvement in precision. Many factors affect soil genesis, and soils present an extraordinary variation in composition and characteristics compared with other environmental materials. This makes it difficult to construct a calibration containing the immense variation found in soils, even at a regional scale (Sudduth & Hummel, 1996; Sankey *et al.,* 2008; Minasny *et al.,* 2009; Reeves & Smith, 2009). In this way, a large calibration does not guarantee accurate predictions. In fact, several authors observed inaccurate predictions when calibrations were used in samples from independent sites (Christy, 2008; D'Acqui *et al.,* 2010; Wetterlind & Stenberg, 2010; Bellon-Maurel & McBratney, 2011). Thus, trying to include all the soil's

variation is an immense and probably unnecessary effort. Spiking could be an attractive and economical alternative, avoiding the need for large spectral libraries, since we observed the best results when the small-sized initial calibration was spiked. As Guerrero *et al.* (2010) observed, the new information added (i.e. the spiking subset) was more influential on a small-sized initial calibration than on a large-sized one, which explains why better predictions were obtained after spiking the small-sized initial calibration (IC#1).

4.2. Effects of extra-weighting on the spiking subset selection strategies

To directly increase the significance or relevance of the added information, several copies of the spiking subset were included in the spiked initial calibrations. The addition of several copies increased their weight and influence on the model (Stork & Kowalski, 1999). Under these circumstances, the calibration was forced to fit preferentially to these samples. Consequently, if the extra-weighted samples are representative of the overall prediction set (i.e. the target site), then the calibration must provide reliable predictions for that set. Indeed, extra-weighting caused a significant improvement ($P < 0.001$) on all the parameters related to the quality of predictions. It is interesting to highlight that the effects on the precision (SEP) and accuracy (RMSEP) were similar for the three initial calibrations evaluated, suggesting a robustness of that pattern, since the three initial calibrations were different to each other. So, extra-weighting is a simple, fast and inexpensive task that we recommend when spiking calibrations. The extra-weighting caused a strong decrease in the leverage of the spiking subset (Stork & Kowalski, 1999; Capron *et al.,* 2005). Consequently, the extra-weighting could be considered as a manipulation of the spectral space, since it causes a displacement of the calibration centroid toward the extra-weighted samples. In this sense, the extra-weighting is a frequent approach used in samples that are added for updating

calibrations to new conditions, especially when their number is relatively low in comparison with the overall calibration set (Stork & Kowalski, 1999), as in our scenarios (especially in IC#2 and IC#3).

The improvement in the RMSEP, SEP and RPD was dependent on the strategy used to select the spiking subset, as Capron *et al.* (2005) also observed. The differences found between strategies were similar in the three initial calibrations used, as revealed by the non-significant interaction ($P > 0.05$) between the 'strategy' and 'initial calibration' factors. These results suggest that the effects exerted by the added samples (spiking subset) are not totally controlled by the characteristics of the initial calibration. The soil samples within a local set are different from each other, the information provided by each sample is different (Naes, 1987; Isaksson & Naes, 1990; Shetty *et al.,* 2012), and consequently, the improvement in the accuracy of the spiked calibration should also vary. In this sense, using an inadequate spiking subset could be one of the reasons explaining why some authors have found a scarce effect of spiking (Bricklemyer & Brown, 2010; Guerrero *et al.,* 2010). Thus, the identification of a successful strategy to select the most adequate spiking subset is clearly relevant. For these reasons, we evaluated strategies aimed to cover a wide range of different types of spiking subset. Since large bias values have been the most common problem observed (Stork & Kowalski, 1999; Janik *et al.,* 2007; Bellon-Maurel & McBratney, 2011), we suspected that using a spiking subset containing strategic SOC values could be adequate to improve the bias, and consequently the accuracy. In fact, we observed that the 'OC tails' and 'OC distrib' selection strategies offered better predictions than the 'OC centre', 'OC high' and 'OC low' strategies, since they were adding information in several strategic spaces related with the bias, slope and offset. But it is important to note

456 that the strategies based on the SOC values are not useful in practice, and they were
457 included in the experiment for conceptual evaluation and comparison.

458 The calibrations spiked with samples evenly distributed in the principal component
459 spectral space ('PC distrib') gave better predictions than those spiked with samples
460 evenly distributed along the concentration values ('OC distrib'). Both strategies select
461 different local samples because the SOC content is not uniquely responsible for the
462 spectral variation within a target site. Compared to texture and mineralogy composition,
463 SOC typically has a fairly small influence on spectra (Stenberg *et al.,* 1995; Islam *et al.,*
464 2005; Stenberg *et al.,* 2010). This result is interesting since only the spectral
465 information is available in a real situation (Kusumo *et al.,* 2008; Mora & Schimleck,
466 2008). The predictions obtained with calibrations spiked with a spiking subset selected
467 using the 'PC centre' strategy were less accurate than those selected with 'PC periph'.
468 The samples selected with the 'PC centre' strategy are those more similar to the mean
469 spectrum of the target site. In contrast, those selected with 'PC periph' are more
470 dissimilar to the mean spectrum, but they represent greater diversity. The strategies that
471 included most of the spectral diversity were 'PC distrib' and 'PC periph', and they were
472 two successful strategies, especially the latter. Indeed, there are several methods for
473 optimal sample selection based on spectral characteristics (Naes, 1987; Puchwein, 1988;
474 Isaksson & Naes, 1990; Shenk & Westerhaus, 1991; Kusumo *et al.,* 2008) but two of
475 the most commonly used are the Kennard–Stone algorithm (Kennard & Stone, 1969;
476 Mora & Schimleck, 2008; Shetty *et al.,* 2012), which covers the experimental region
477 uniformly (as in 'PC distrib'), and the D-optimal procedure (Olsson *et al.,* 2004;
478 Rodionova & Pomerantsev, 2007; Brandmaier *et al.,* 2012), which selects objects
479 located on the periphery (most extreme) of the experimental region (as in 'PC periph').

There were scarce differences between the selections made using the Mahalanobis distance. The values of Mahalanobis distance were extremely high, and all the local samples were always classified as outliers. Consequently, these sets are not sensitive to the Mahalanobis distance criterion. This criterion would probably be relevant when samples from the target sites are more similar to those comprising the initial calibration (Puchwein, 1988; Capron *et al.,* 2005).

4.3. Increase of spiking subset size versus extra-weighting, and comparison with geographically local models

When the 'PC distrib' strategy was used to select the spiking subset, extra-weighting was preferred over the increase in spiking subset size. This was a very interesting result, since extra-weighting caused a significant improvement inaccuracy without any analytical effort. In contrast, the increase of the spiking subset size implies efforts in terms of time and money, and the improvement of the RMSEP was not statistically significant. The non-significant improvement of the RMSEP was probably due to the high efficiency of the 'PC distrib' strategy to select the most representative samples. Consequently, a further addition of samples would prove scarcely useful, since the new added samples would be redundant (in comparison with the first ones selected). These results agree with those obtained by other authors (Naes, 1987; Puchwein, 1988; Isaksson & Næs, 1990; Capron *et al.,* 2005; D'Acqui *et al.,* 2010; Grinand *et al.,* 2012; Shetty *et al.,* 2012), where only a small subset of samples properly selected can offer a similar accuracy than a larger set. In this context, extra-weighting the spiking subset is an efficient approach, which can avoid the need of large-sized spiking subsets.

The influence of spiking was greater in the small-sized initial calibrations than in the large-sized ones (Guerrero *et al.,* 2010). When the extra-weighting was made using the same number of copies regardless of the initial calibration size (EW_24), this

505 pattern was still present, but clearly to a lesser degree. When the extra-weighting was
506 based on the initial calibration to spiking subset ratio (EW_ratio), more copies were
507 included in the large-sized initial calibration (IC#3) than in the smaller-sized initial
508 calibrations (IC#1 and IC#2). However, even under these conditions, the results
509 obtained for the three initial calibrations were similar. This result was very interesting
510 because it suggests that small-sized initial calibrations could offer a similar accuracy
511 than large-sized initial calibrations. Consequently, this approach can be considered as a
512 strong alternative to the need to develop large spectral libraries. In addition, in those
513 circumstances where only a few local samples can be analysed by the reference method
514 (i.e. 8–16 samples), this approach offered more accurate results than the geographically
515 local (or site-specific) models. When a larger number of local samples were analysed
516 (32 local samples), small differences in accuracy were observed between both
517 approaches, although the geographically local models were less robust, indicating the
518 difficulty to develop consistent spectroscopic calibrations when the number of samples
519 is low.

520 More studies are needed to evaluate if extra-weighting can outperform local models
521 (spectrum-specific models), where a dedicated model is calibrated for an individual
522 unknown sample (Pérez-Marín *et al.,* 2007), or other approaches where a partition of
523 the spectral information is used (Viscarra Rossel & Webster, 2012). It is interesting to
524 highlight that local methods (spectrum-specific) can be used only when the spectral
525 library contains similar samples to the target site samples, which is not the case for sets
526 evaluated in this paper. In contrast, spiking with a properly selected spiking subset,
527 together with extra-weighting, can overcome this problem, allowing the extrapolation of
528 the initial calibrations applicability.

529

Conclusions

The addition of a small spiking subset (eight local samples) to spike the calibrations improved the accuracy of the SOC predictions. There were, however, important differences in accuracy, which were dependent on the strategy used to select the spiking subset. The best results were obtained when the calibrations were spiked with local samples that were evenly distributed across the space defined by the first three principal components (spiking subset selected with the 'PC distrib' strategy). In addition, extra-weighting was an effective way to improve the accuracy of the spiked calibrations. Extra-weighting of the spiking subset accentuates the spiking effect, giving an acceptable level of accuracy when predictions of SOC are needed at local scale, and when using small-sized spiking subsets. Large-sized calibrations are probably not needed when these approaches are considered, since similar results were obtained with the small- and large-sized calibrations, and it suggests that incipient spectral libraries could be useful if they are properly spiked and extra-weighted. Consequently, extra-weighting is a simple, fast and inexpensive task that we highly recommend when calibrations are spiked, and can avoid the need to develop geographically local models. Overall, our results indicate that the efforts needed to use NIR spectroscopy for SOC assessment at local scales can be minimised.

Acknowledgements

This work was part of a research project (Ref. CGL2011-27001) sponsored by the Spanish Government Ministerio de Economía y Competitividad, and C. Guerrero gratefully acknowledges this financial support. C. Guerrero acknowledges the Spanish Government Ministerio de Educación for a travel grant (ref. JC2011-0342). F.T. Maestre was supported by the European Research Council through the European

554 Commission's Seventh Framework Programme (FP7/2007–2013) under grant
555 agreement no. 242658 (BIOCOM).

556

References

Bellon-Maurel, V. & McBratney, A. 2011. Near-infrared (NIR) and mid-infrared (MIR) spectroscopic techniques for assessing the amount of carbon stock in soils – Critical review and research perspectives. *Soil Biology and Biochemistry*, **43**, 1398–1410.

Brandmaier, S., Sahlin, U., Tetko, I.V. & Oberg, T. 2012. PLS-Optimal: A stepwise D-Optimal design based on latent variables. *Journal of Chemical Information and Modeling*, **52**, 975–983.

Bricklemyer, R.S. & Brown, D.J. 2010. On-the-go VisNIR: Potential and limitations for mapping soil clay and organic carbon. *Computers and Electronics in Agriculture*, **70**, 209–216.

Brown, D.J. 2007. Using a global VNIR soil-spectral library for local soil characterization and landscape modelling in a 2nd-order Uganda watershed. *Geoderma*, **140**, 444–453.

Brown, D.J., Bricklemyer, R.S. & Millar, P.R. 2005. Validation requirements for diffuse reflectance soil characterization models with a case study of VNIR soil C prediction in Montana. *Geoderma*, **129**, 251–267.

Brown, D.J., Shepherd, K.D., Walsh, M.G., Mays, M.D. & Reinsch, T.G. 2006. Global soil characterization with VNIR diffuse reflectance spectroscopy. *Geoderma*, **132**, 273–290.

Capron, X., Walczak, B., de Noord, O.E. & Massart, D.L. 2005. Selection and weighting of samples in multivariate regression model updating. *Chemometrics and Intelligent Laboratory Systems*, **76**, 205–214.

579 Christy, C.D. 2008. Real-time measurement of soil attributes using on-the-go near
580 infrared reflectance spectroscopy. *Computers and Electronics in Agriculture*, **61**,
581 10–19.

582 D'Acqui, L.P., Pucci, A. & Janik, L.J. 2010. Soil properties prediction of western
583 Mediterranean islands with similar climatic environments by means of mid-infrared
584 diffuse reflectance spectroscopy. *European Journal of Soil Science*, **61**, 865–876.

585 Genot, V., Colinet, G., Bock, L., Vanvyve, D., Reusen, Y. & Dardenne, P. 2011. Near
586 infrared reflectance spectroscopy for estimating soil characteristics valuable in the
587 diagnosis of soil fertility. *Journal of Near Infrared Spectroscopy*, **19**, 117–138.

588 Gogé, F., Joffre, R., Jolivet, C., Ross, I. & Ranjard, L. 2012. Optimization criteria in
589 sample selection step of local regression for quantitative analysis of large soil NIRS
590 database. *Chemometrics and Intelligent Laboratory Systems*, **110**, 168–176.

591 Grinand, C., Barthès, B.G., Brunet, D., Kouakoua, E., Arrouays, D., Jolivet, C., Caria,
592 G. & Bernoux, M. 2012. Prediction of soil organic and inorganic carbon contents at
593 a national scale (France) using mid-infrared reflectance spectroscopy (MIRS).
594 *European Journal of Soil Science*, **63**, 141–151.

595 Guerrero, C., Zornoza, R., Gómez, I. & Mataix-Beneyto, J. 2010. Spiking of NIR
596 regional models using simples from target sites: Effect of model size on prediction
597 accuracy. *Geoderma*, **158**, 66–77.

598 Isaksson, T. & Naes, T. 1990. Selection of samples for calibration in near-infrared
599 spectroscopy. Part II: selection based on spectral measurements. *Applied*
600 *Spectroscopy*, **44**, 1152–1158.

Islam, K., McBratney, A. & Singh, B. 2005. Rapid estimation of soil variability from the convex hull biplot area of topsoil ultra-violet, visible and near-infrared diffuse reflectance spectra. *Geoderma*, **128**, 249–257.

Janik, L.J., Skjemstad, J.O., Sheperd, K.D. & Spouncer, L.R. 2007. The prediction of soil carbon fractions using mid-infrared-partial least square analysis. *Australian Journal of Soil Research*, **45**, 73–81.

Kennard, R.W. & Stone, L.A. 1969. Computer aided design of experiments. *Technometrics*, **11**, 137–148.

Kuang, B. & Mouazen, A.M. 2013. Effect of spiking strategy and ratio on calibration of on-line visible and near infrared soil sensor for measurement in European farms. *Soil & tillage Research*, **128**, 125–136.

Kusumo, B.H., Hedley, C.B., Hedley, M.J., Hueni, A., Tuohy, M.P. & Arnold, G.C. 2008. The use of diffuse reflectance spectroscopy for in situ carbon and nitrogen analysis of pastoral soils. *Australian Journal of Soil Research*, **46**, 623-635.

Minasny, B., Tranter, A.B., Brough, D.M. & Murphy, B.W. 2009. Regional transferability of mid-infrared diffuse reflectance spectroscopic prediction for soil chemical properties. *Geoderma*, **153**, 155–162.

Mora, C.R. & Schimleck, L.R. 2008. On the selection of samples for multivariate regression analysis: application to near-infrared (NIR) calibration models for the prediction of pulp yield in Eucalyptus nitens. *Canadian Journal of Forest Research*, **38**, 2626–2634.

Naes, T. 1987. The design of calibration in near infrared reflectance analysis by clustering. *Journal of Chemometrics*, **1**, 121–134.

624 Olsson, I-M., Gottfries, J. & Wold, S. 2004. D-optimal onion designs in statistical
625 molecular design. *Chemometrics and Intelligent Laboratory Systems*, **73**, 37–46.
626 Pérez-Martín, D., Garrido-Varo, A. & Guerrero, J.E. 2007. Non-linear regression
627 method in NIRS quantitative analysis. *Talanta*, **72**, 28–42.
628 Puchwein, G. 1998. Selection of calibration samples for near-infrared spectrometry by
629 factor analysis of spectra. *Analytical Chemistry*, **60**, 569–573.
630 Reeves III, J.B., McCarty, G.W. & Meisinger, J.J. 1999. Near infrared reflectance the
631 analysis of agricultural soils. *Journal of Near Infrared Spectroscopy*, **7**, 179–193.
632 Reeves III, J.B. & Smith, D.B. 2009. The potential of mid- and near-infrared diffuse
633 reflectance spectroscopy for determining major- and trace-element concentrations
634 in soils from a geochemical survey of North America. *Applied Geochemistry*, **24**,
635 1472–1481.
636 Rodionova, O.Y. & Pomerantsev, A.L. 2008. Subset selection strategy. *Journal of*
637 *Chemometrics*, **22**, 674–685.
638 Sankey, J.B., Brown, D.J., Bernard, M.L. & Lawrence, R.L. 2008. Comparing local vs.
639 global visible and near-infared (VisNIR) diffuse reflectance spectroscopy (DRS)
640 calibrations for the prediction of soil clay, organic C and inorganic C. *Geoderma*,
641 **148**, 149–158.
642 Shenk, J.S. & Westerhaus, M.O. 1991. Population definition, sample selection, and
643 calibration procedures for near-infrared reflectance spectroscopy. *Crop Science*, **31**,
644 469–474.
645 Shepherd, K.D. & Walsh, M.G. 2002. Development of reflectance spectral libraries for
646 characterization of soil properties. *Soil Science Society of America Journal*, **66**,
647 988–998.

Shetty, N., Rinnan, A. & Gislum, R. 2012. Selection of representative calibration sample sets for near-infrared reflectance spectroscopy for predict nitrogen concentration in grasses. *Chemometrics and Intelligent Laboratory Systems*, **111**, 59–65.

Stenberg, B., Nordkvist, E. & Salomonsson, L. 1995. Use of near infrared reflectance spectra of soils for objective selection of samples. *Soil Science*, **159**, 109–114.

Stenberg, B., Viscarra Rossel, R.A., Mouazen, A.M. & Wetterlind, J. 2010. Visible and near infrared spectroscopy in soil science. *Advances in Agronomy*, **107**, 163–215.

Stork, C.L. & Kowalski, B.R. 1999. Weighting schemes for updating regression models – a theoretical approach. *Chemometrics and Intelligent Laboratory Systems*, **48**, 151–166.

Sudduth, K.A. & Hummel, J.W. 1996. Geographical operating range evaluation of a NIR soil sensor. *Transactions of the ASAE*, **39**, 1599–1604.

Viscarra Rossel, R.A. & Webster, R. 2012. Predicting soil properties from the Australian soil visible-near infrared spectroscopic database. *European Journal of Soil Science*, **63**, 848–860.

Viscarra Rossel, R. 2009. The Soil Spectroscopy Group and the development of a global soil spectral library. *NIR News*, **20**, 14–15.

Viscarra Rossel, R.A., Jeon, Y.S., Odeh, I.O.A. & McBratney A.B. 2008. Using a legacy soil sample to develop a mid-IR spectral library. *Australian Journal of Soil Research*, **46**, 1–16.

Viscarra Rossel, R.A., Cattle, S.R., Ortega, A. & Fouad, Y. 2009. In situ measurements of soil colour, mineral composition and clay content by vis-NIR spectroscopy. *Geoderma*, **150**, 253–266.

672 Walkley, A. & Black, I.A. 1934. An examination of the Degtjareff method for
673 determining soil O.M. and a proposed modification of the chromic acid titration
674 method. *Soil Science*, **37**, 29–38.

675 Wetterlind, J. & Stenberg, B. 2010. Near-infrared spectroscopy for within-field soil
676 characterization: small local calibrations compared with national libraries spiked
677 with local samples. *European Journal of Soil Science*, **61**, 823–843.

678 Wetterlind, J., Stenberg, B. & Söderström, M. 2010. Increased sample point density in
679 farm soil mapping by local calibration of visible and near infrared prediction
680 models. *Geoderma*, **156**, 152–160.

681

682

683 **FIGURE CAPTIONS**

684

685 **Figure 1** Projections of the NIR spectra from the target sites (TS) into the principal
686 component space defined by the first two principal components, in each initial
687 calibration (IC). Grey stars denote the national samples of the initial calibrations and
688 black dots denote target site samples.

689

690 **Figure 2** Schematic description of the experimental setup: a) initial calibration (IC)
691 unspiked, constructed only with national samples (NS); b) initial calibration spiked with
692 a spiking subset (SS) selected by strategy #1; c) initial calibration spiked with spiking
693 subset selected by strategy #1, where an extra-weighting was applied to the spiking
694 subset. This scheme only shows one of the 13 strategies of spiking subset selection and
695 one of the three initial calibrations. This scheme was used with four different target sites
696 (TS). Dashed and double lines denote spiking and the use of the calibration for
697 obtaining predictions ($\hat{y}$), respectively.

698

699 **Figure 3a** Representative illustration of predictions obtained in each target site (TS)
700 with the different calibrations conducted. Left: predictions obtained with the unspiked
701 IC#1 (white stars; dotted line). Centre: predictions obtained with IC#1 spiked with the
702 spiking subset selected with the 'MD centre' strategy (white circles, dashed line) and
703 spiking subset extra-weighted (EW) (black circles, solid line). Right: predictions
704 obtained with IC#1 spiked with the spiking subset selected with the 'PC distrib' strategy
705 (white circles, dashed line) and spiking subset extra-weighted (black circles, solid line).

706

Figure 3b Representative illustration of predictions obtained in each target site (TS) with the different calibrations conducted. Left: predictions obtained with the unspiked IC#2 (white stars; dotted line). Centre: predictions obtained with IC#2 spiked with the spiking subset selected with the 'MD centre' strategy (white circles, dashed line) and spiking subset extra-weighted (EW) (black circles, solid line). Right: predictions obtained with IC#2 spiked with the spiking subset selected with the 'PC distrib' strategy (white circles, dashed line) and spiking subset extra-weighted (black circles, solid line).

Figure 3c Representative illustration of predictions obtained in each target site (TS) with the different calibrations conducted. Left: predictions obtained with the unspiked IC#3 (white stars; dotted line). Centre: predictions obtained with IC#3 spiked with the spiking subset selected with the 'MD centre' strategy (white circles, dashed line) and spiking subset extra-weighted (EW) (black circles, solid line). Right: predictions obtained with IC#3 spiked with the spiking subset selected with the 'PC distrib' strategy (white circles, dashed line) and spiking subset extra-weighted (black circles, solid line).

Figure 4 Predictions obtained with unspiked and spiked calibrations (without and with extra-weight) using the 13 different strategies to select the spiking subset. Strategies in spiked calibrations (with and without extra-weighting) are arranged by RMSEP. a) IC#1; b) IC#2; c) IC#3. In all cases, n = 4 (from the four target sites studied). The two horizontal dark grey lines are displaying values of RMSEP = 0.4% soil organic carbon (SOC) and RMSEP = 0.8% SOC to facilitate visual comparisons.

731 **Figure 5** Values of the root mean square error of prediction (RMSEP) obtained with the
732 three initial calibrations (IC) spiked with a spiking subset (SS) of size 8 (SS8), 16
733 (SS16) and 32 (SS32), without extra-weight (black bars), and with extra-weight (EW;
734 grey bars). Dark-grey bars are used when 24 copies of the spiking subset were added for
735 extra-weighting (EW_24), and light-grey bars are used when the numbers of copies
736 were added in proportion of the initial calibration to spiking subset ratio (EW_ratio).
737 White bars and horizontal lines were used to show the RMSEP obtained with
738 geographically local models, constructed uniquely with 8 (horizontal dotted line), 16
739 (horizontal dashed line) or 32 local samples (horizontal solid line). In all the cases, the
740 local samples were selected by the 'PC distrib' strategy. In all the cases n = 4 (from four
741 target sites). The error bars are denoting one standard deviation.
742
743

744

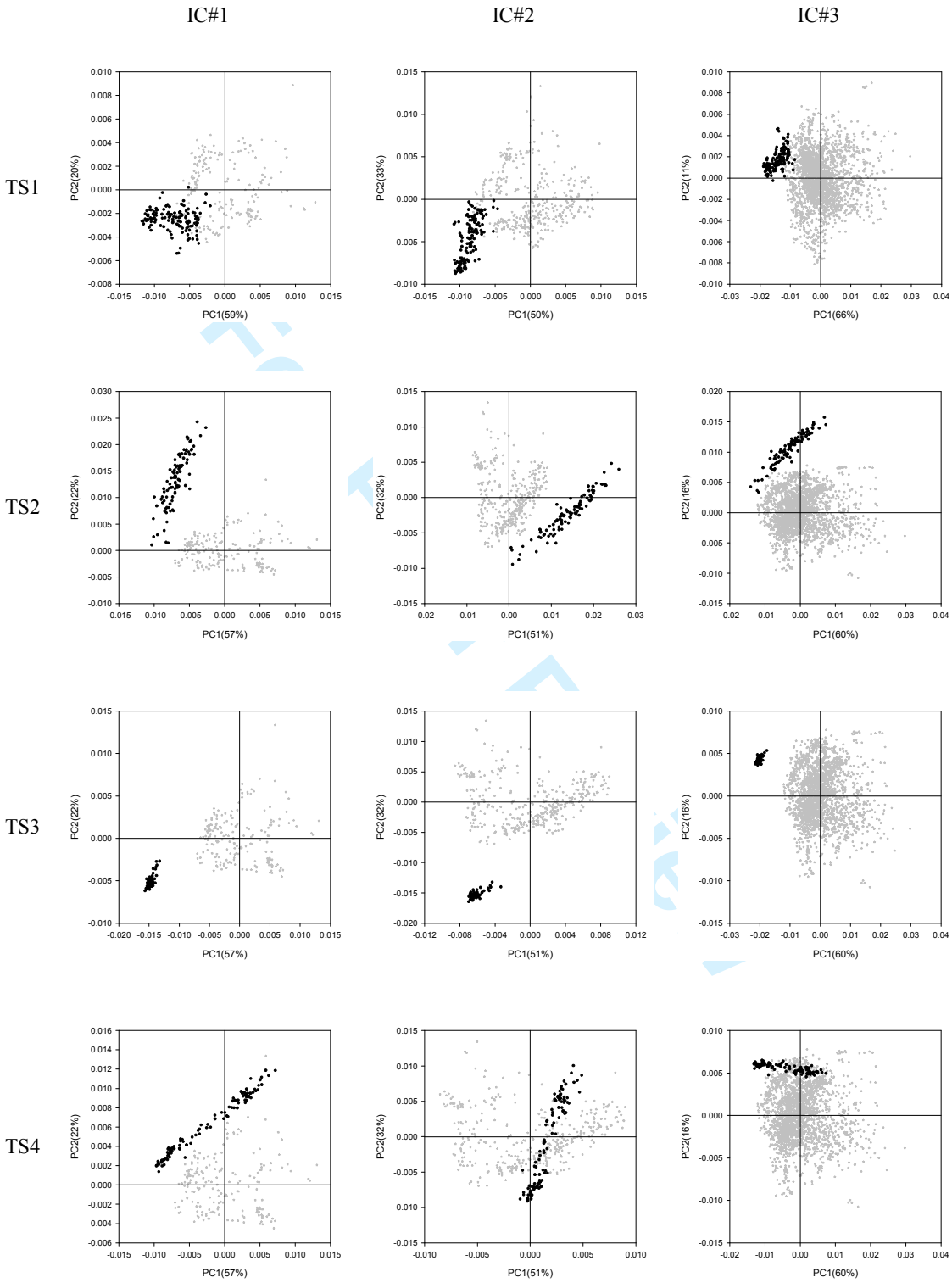

745 **Figure 1**

746

747

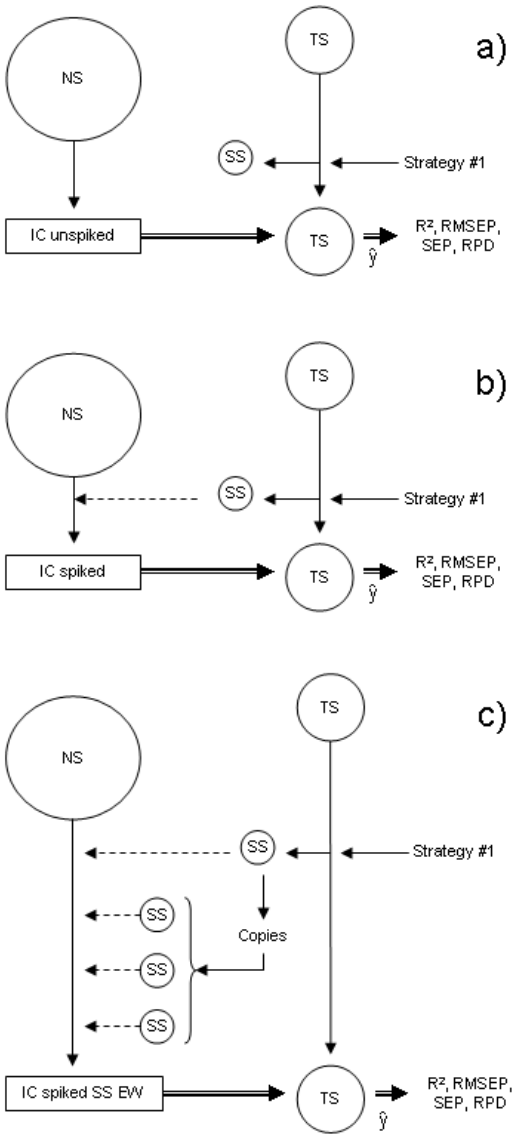

748

749 **Figure 2**

750

751

752

753

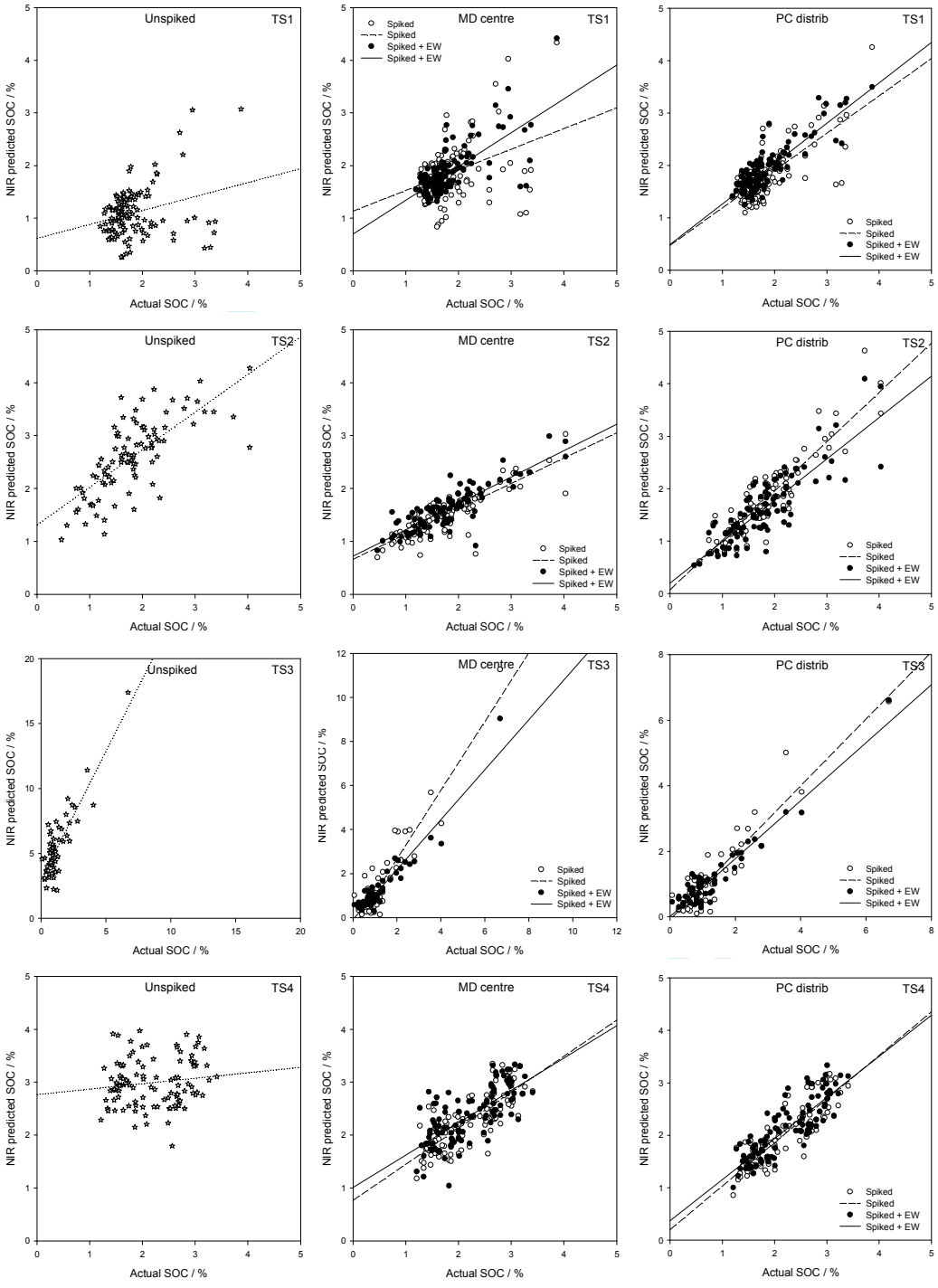
Unspiked TS1
MD centre TS1
PC distrib TS1
Unspiked TS2
MD centre TS2
PC distrib TS2
Unspiked TS3
MD centre TS3
PC distrib TS3
Unspiked TS4
MD centre TS4
PC distrib TS4
Spiked
Spiked
Spiked + EW
Spiked + EW
NIR predicted SOC / %
Actual SOC / %

Figure 3a

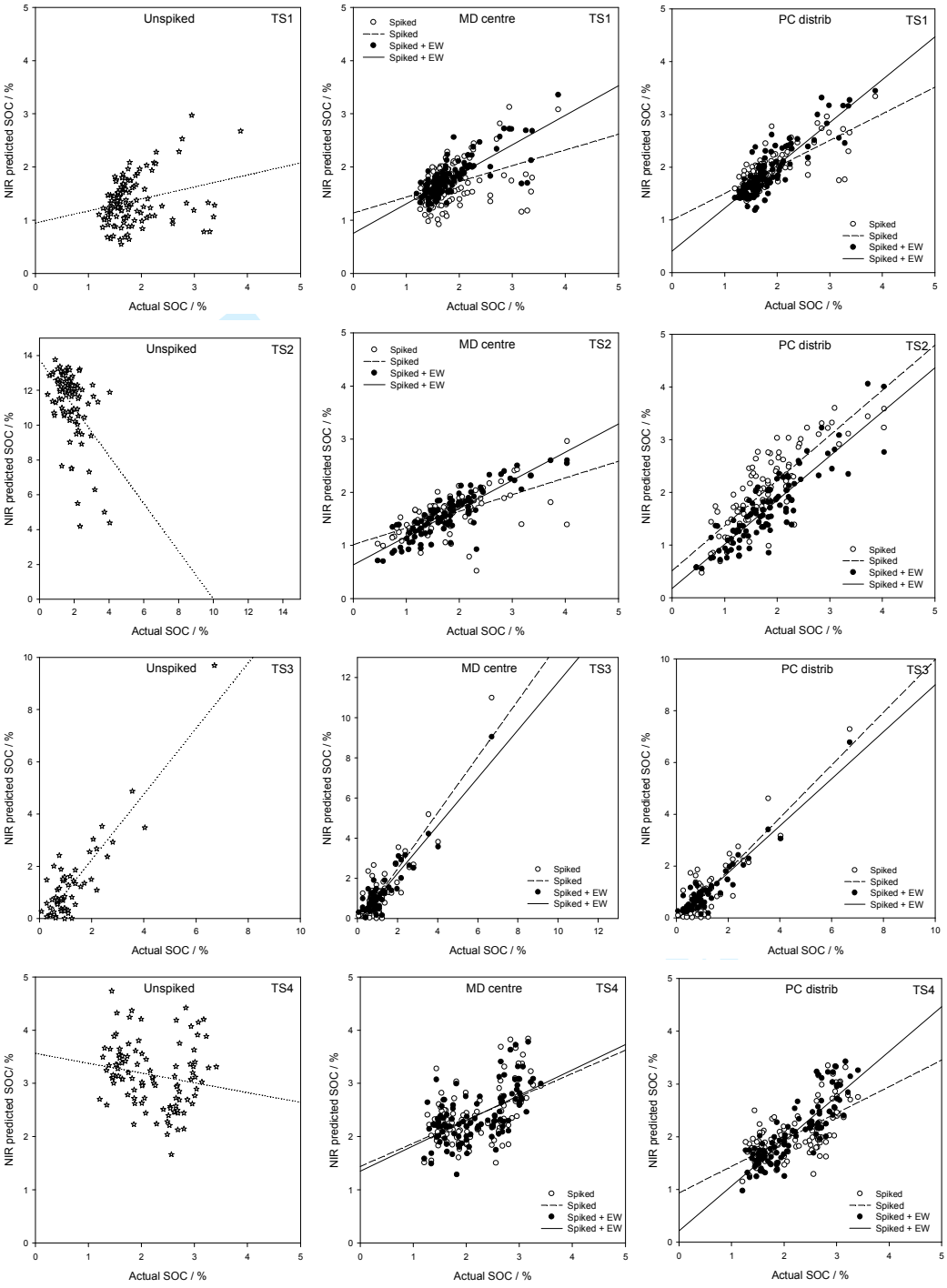
Unspiked
TS1
MD centre
TS1
PC distrib
TS1
Unspiked
TS2
MD centre
TS2
PC distrib
TS2
Unspiked
TS3
MD centre
TS3
PC distrib
TS3
Unspiked
TS4
MD centre
TS4
PC distrib
TS4
Spiked
Spiked
Spiked + EW
Spiked + EW
NIR predicted SOC / %
Actual SOC / %

Figure 3b

768

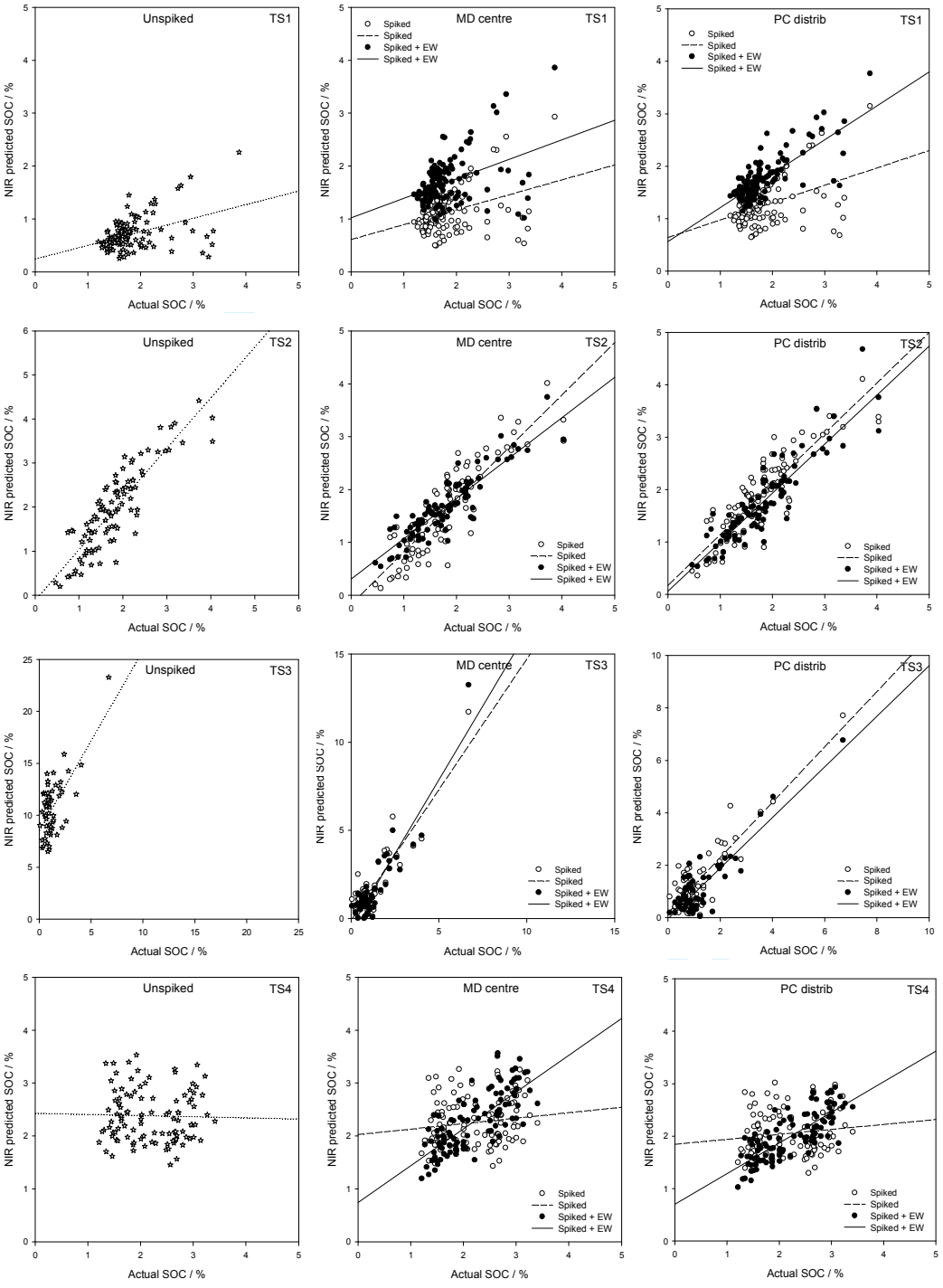

769

770

771

772

773 **Figure 3c**

774

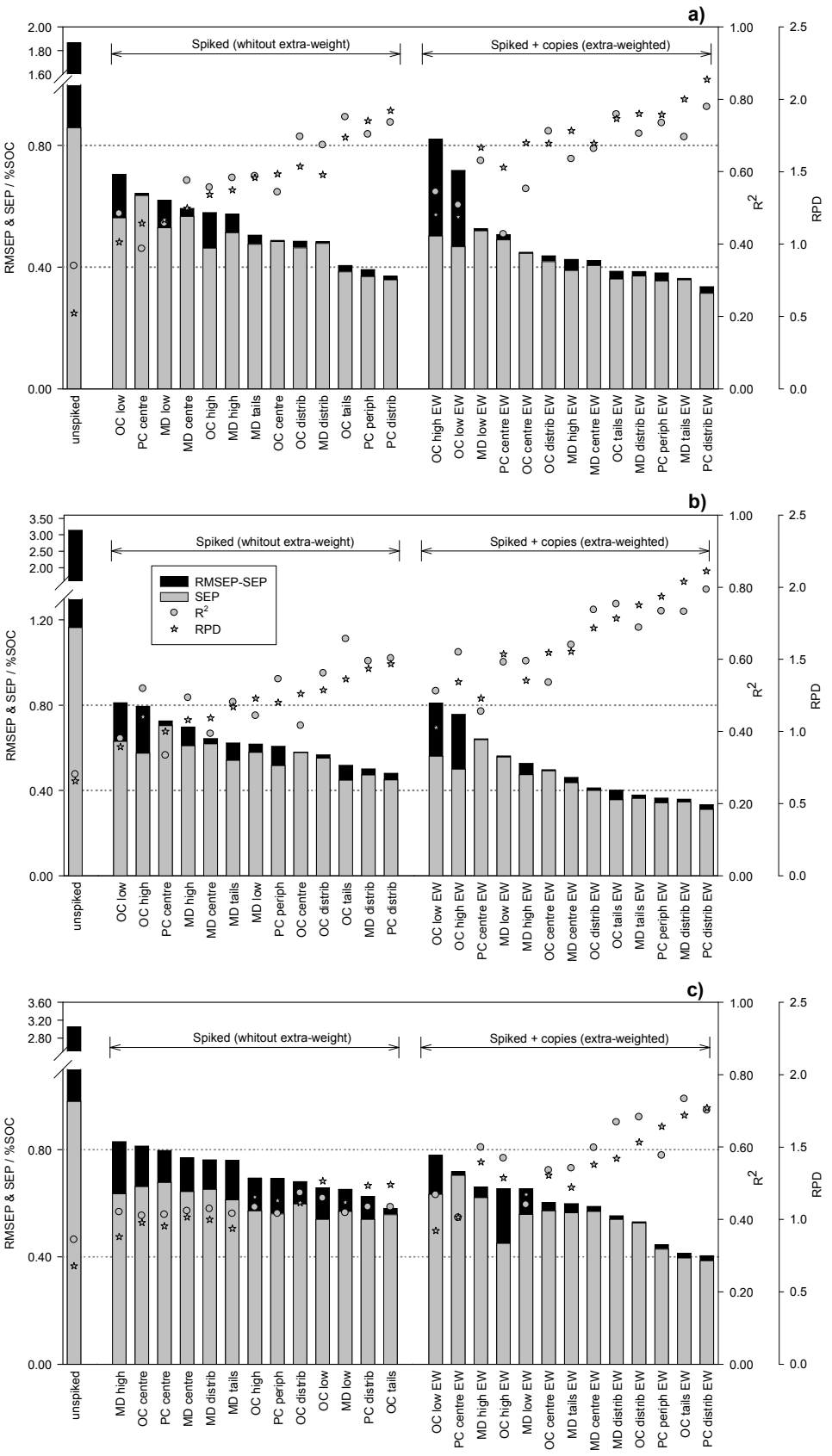
a)
Spiked (whitout extra-weight)
Spiked + copies (extra-weighted)
RMSEP & SEP / %SOC
R2
RPD
unspiked
OC low
PC centre
MD low
MD centre
OC high
MD high
MD tails
OC centre
OC distrib
MD distrib
OC tails
PC periph
PC distrib
OC high EW
OC low EW
MD low EW
PC centre EW
OC centre EW
OC distrib EW
MD high EW
MD centre EW
OC tails EW
MD distrib EW
PC periph EW
MD tails EW
PC distrib EW
b)
RMSEP-SEP
SEP
R2
RPD
c)

Figure 4

779

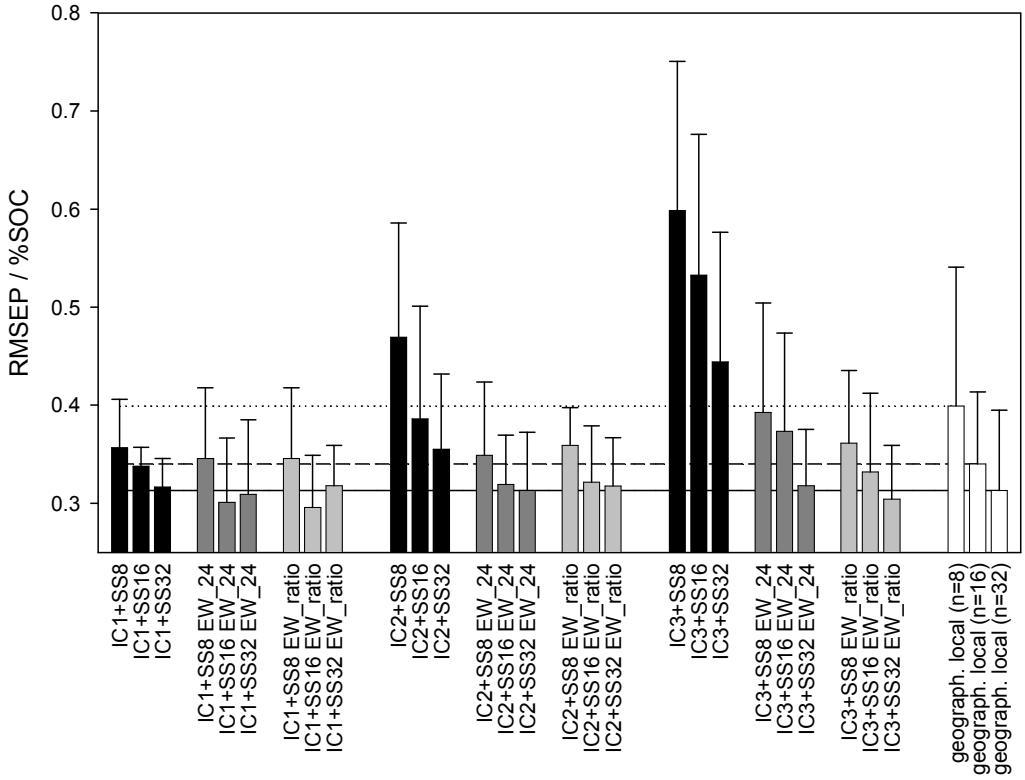

780

781 **Figure 5**

782

783

784

TABLES

Table 1 Characteristics of the three subsets used for the development of the different Initial Calibrations (ICs), and the coefficient of determination (R^2) and root mean square error (RMSE) obtained in the cross-validations (RMSECV). All the results refer to soil organic carbon (in %).

	IC #1	IC #2	IC #3
n	192	365	2279
Minimum	0.32	0.32	0.10
Maximum	8.97	14.49	14.62
Mean	2.35	5.07	1.54
Standard deviation	1.87	3.59	2.14
Skewness	1.05	0.41	3.20
R^2	0.95	0.96	0.93
RMSECV	0.40	0.67	0.54

793 **Table 2** Characteristics of the four target sites used. Data refer in all cases to soil organic carbon (SOC; %).

794

	Target site 1	Target site 2	Target site 3	Target site 4
Coordinates	55º41'N, 13º19'E	38º32'N, 0º49'W	37º09'N, 2º35'W	52º00'N, 0º26'W
Site (country)	Sjöstorp (Sweden)	Sax (Spain)	Gergal (Spain)	Silsoe (UK)
Parent material	Sandy till (25%) and sedimentary clay with elements of chalk (75%)	Gypsum	Mica schists	Mudstone
Method SOC	LOI[a] (900ºC)	Elemental Analyser	Walkley & Black	LOI (900ºC)
Spectral range / nm	1000-2500	834-2650	834-2650	834-2650
n	125	95	60	104
Minimum	1.20	0.47	0.07	1.21
Maximum	3.87	4.04	6.70	3.41
Mean	1.83	1.80	1.23	2.20
Standard deviation	0.50	0.71	1.05	0.60

795 [a] LOI: loss on ignition

796

797

Table 3 Results of the repeated measures ANOVA to evaluate the effects of extra-weighting, initial calibration and strategy on the different prediction performance parameters: root mean square error of prediction (RMSEP), standard error of prediction (SEP) and ratio of performance to deviance (RPD).

Variable		Source	Sum of squares	Degrees of freedom	Mean square	F	*P*
RMSEP[a]	Between-subjects	Initial Calibration (IC)	0.605	2	0.302	11.84	0.0000
	Between-subjects	Strategy	0.701	7	0.100	3.918	0.0011
	Between-subjects	IC × Strategy	0.078	14	0.005	0.220	0.9985
	Between-subjects	Error	1.840	72	0.025		
	Within-subjects	Extra-weighting (EW)	0.668	1	0.668	81.90	0.0000
	Within-subjects	EW × IC	0.015	2	0.007	0.956	0.3890
	Within-subjects	EW × Strategy	0.045	7	0.006	0.794	0.5940
	Within-subjects	EW × IC × Strategy	0.085	14	0.006	0.751	0.7165
	Within-subjects	Error (EW)	0.587	72	0.008		
SEP[b]	Between-subjects	IC	1.872	2	0.936	6.593	0.0023
	Between-subjects	Strategy	3.760	7	0.537	3.782	0.0015
	Between-subjects	IC × Strategy	0.420	14	0.030	0.211	0.9988
	Between-subjects	Error	10.22	72	0.142		
	Within-subjects	EW	2.125	1	2.125	60.76	0.0000
	Within-subjects	EW × IC	0.126	2	0.063	1.801	0.1725
	Within-subjects	EW × Strategy	0.235	7	0.033	0.959	0.4673
	Within-subjects	EW × IC × Strategy	0.306	14	0.021	0.626	0.8346
	Within-subjects	Error (EW)	2.518	72	0.035		
RPD[b]	Between-subjects	IC	3.209	2	1.604	7.372	0.0012
	Between-subjects	Strategy	3.716	7	0.531	2.439	0.0266
	Between-subjects	IC × Strategy	0.417	14	0.029	0.137	0.9999
	Between-subjects	Error	15.67	72	0.217		
	Within-subjects	EW	3.543	1	3.543	81.90	0.0000
	Within-subjects	EW × IC	0.082	2	0.041	0.956	0.3890
	Within-subjects	EW × Strategy	0.240	7	0.034	0.794	0.5940
	Within-subjects	EW × IC × Strategy	0.454	14	0.032	0.751	0.7165
	Within-subjects	Error (EW)	3.114	72	0.043		

[a] Log transformed

[b] Ln transformed

804 **Table 4.** Results of the repeated measures ANOVAs to evaluate the effects of the spiking subset size (SS-size), and those of the extra-weighting (EW) on the
805 root mean square error of prediction (RMSEP) obtained with spiked calibrations. (a) Results obtained when 24 copies where used for EW (EW_24). (b)
806 Results obtained when the number of copies to add for EW was equal to the ratio between the IC size and the SS size (EW_ratio).
807

		Source	Sum of squares	Degrees of freedom	Mean square	F	*P*
(a)	Between-subjects	SS-size	0.0696	2	0.0348	2.328	0.1133
	Between-subjects	Error	0.4936	33	0.0149		
	Within-subjects	EW_24	0.1341	1	0.1341	21.28	0.0000
	Within-subjects	EW_24 × SS-size	0.0087	2	0.0043	0.695	0.5058
	Within-subjects	Error	0.2079	33	0.0063		
(b)	Between-subjects	SS-size	0.0649	2	0.0324	3.117	0.0575
	Between-subjects	Error	0.3437	33	0.0104		
	Within-subjects	EW_ratio	0.1578	1	0.1578	18.45	0.0001
	Within-subjects	EW_ratio × SS-size	0.0119	2	0.0059	0.695	0.5058
	Within-subjects	Error	0.2821	33	0.0085		

808
809

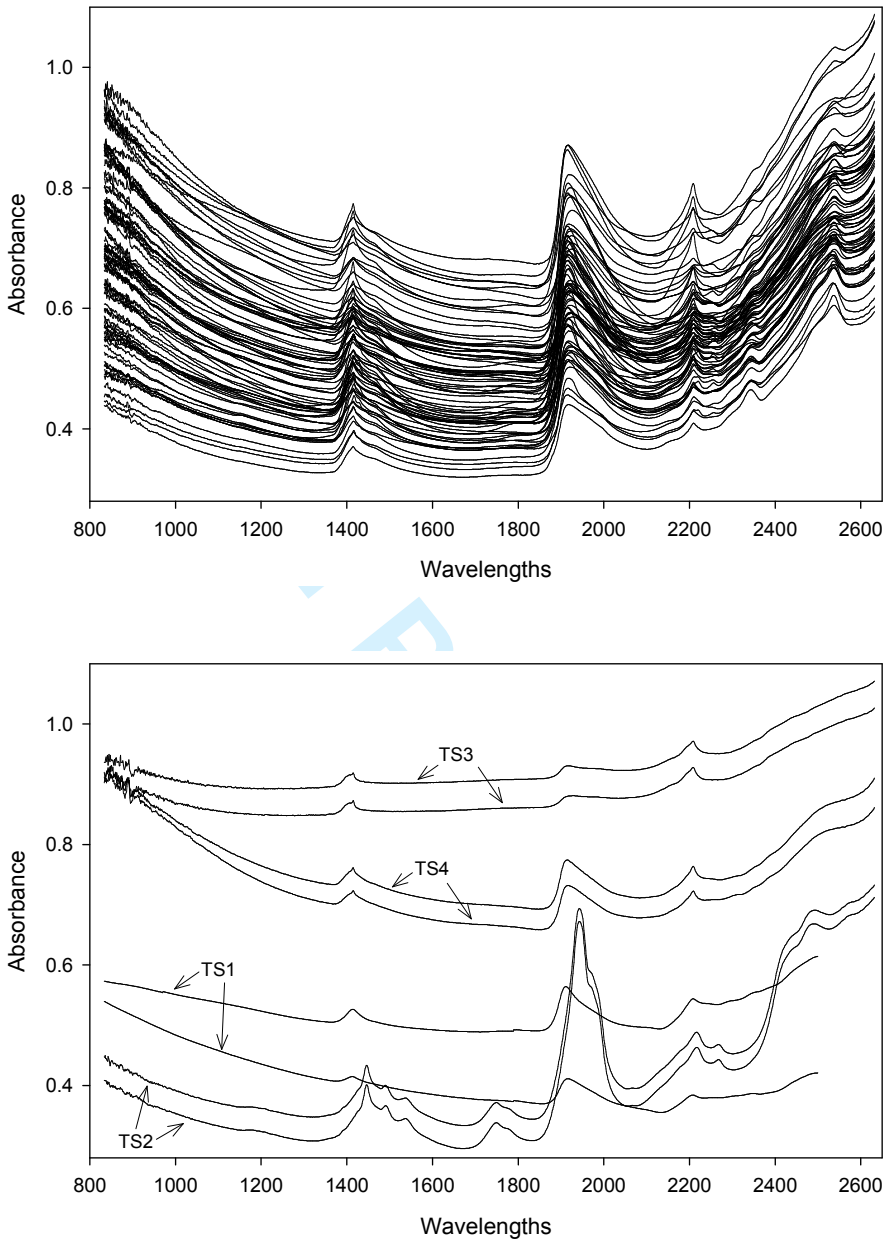

Supplementary content: **Appendix I.** Representative NIR spectra of the national samples included in the initial calibrations (top), and two representative NIR spectra of each of the four target sites (bottom).